DOI: 10.1070/RCR4751

Luminescent carbon nanoparticles: synthesis, methods of investigation, applications

Alina A. Kokorina,[a*] Ekaterina S. Prikhozhdenko,[a*] Gleb B. Sukhorukov,[a, b] Andrei V. Sapelkin,[a, b] Irina Yu. Goryacheva [a]

[a] *Saratov State University*
ul. Astrakhanskaya 83, 410012 Saratov, Russian Federation
[b] *Queen Mary University of London*
Mile End Road, London, E1 4NS, United Kingdom

Luminescent carbon nanoparticles represent a new class of photoluminescent nanomaterials. Growing interest in these nanoparticles stems from straightforward methods of their synthesis, a wide variety of available precursors, the lack of toxicity, photo stability and simple surface modification for further application. Due to low cytotoxicity and tunable optical properties of carbon nanoparticles, they are used in various fields of biology and medicine. At the same time, current application of carbon nanoparticles is limited by the lack of understanding of the fundamental relationship between their structure and properties. The review focuses on the latest trends in the synthesis, study of the structure, composition and properties of carbon nanoparticles and on their biomedical applications.
The bibliography includes 112 references.

Contents

I. Introduction 1157
II. Methods of synthesis 1158
III. Study of properties 1161
IV. Application in biology and medicine 1166
V. Conclusion 1169

I. Introduction

Carbon nanomaterials, which have a wide range of unique properties, have long attracted the attention of the scientific community. This is largely due to the broad prospects for the application of these materials in various fields, especially in biology and medicine. Modern technical capabilities have made it possible to create forms of carbon nanomaterials with different properties. For a long time, carbon nanomaterials have been represented by nanodiamonds, fullerenes and carbon nanotubes.[1, 2]

Fullerenes are convex polyhedra consisting of an even number of three-coordinate carbon atoms. Solid fullerenes exhibit semiconducting properties. They can be used in studying superconductors, and can also be used to introduce certain metal ions such as Gd^{3+}, which leads to the production of contrast agents for magnetic resonance and nuclear medicine.[3] Surface-functionalized fullerenes are used as drug carriers, ensuring slow-release drug delivery, which increases the efficiency of treatment.[4]

* The authors made the same contribution to the writing of the review.

A.A.Kokorina. Associate Researcher at the SSU.
E-mail: alina.gvozdyuk@gmail.com
Current research interests: nanoparticles, luminescence, analytical chemistry, organic chemistry.
E.S.Prikhozhdenko. Associate Researcher at the SSU.
E-mail: prikhozhdenkoes@gmail.com
Current research interests: nanoparticles, theranostics, microcapsules, SERS.
G.B.Sukhorukov. PhD in Physics and Mathematics, Professor at the SSU and the Queen Mary University of London.
E-mail: g.sukhorukov@qmul.ac.uk
Current research interests: theranostics, microcapsules, targeted drug delivery, visualization.
A.V.Sapelkin. Senior Lecturer at the Queen Mary University of London, Engineer at the SSU.
E-mail: a.sapelkin@qmul.ac.uk
Current research interests: nanoparticles, photoluminescence, SERS, quantum dots.
I.Yu.Goryacheva. Doctor in Chemistry, Professor at the SSU.
E-mail: goryachevaiy@mail.ru
Current research interests: nanoparticles, analytical chemistry, luminescence.

Received 4 May 2017
Translation: G.A.Kirakosyan

© 2017 Russian Academy of Sciences and Turpion Ltd.

Nanodiamonds are carbon nanomaterials with unique chemical, optical and mechanical properties. They have a diamond-like crystal lattice with a great number of surface defects.[5] Nanodiamonds exhibit bright photoluminescence and are photostable[6] and biocompatible, so that they can be used for biolabelling.[7,8]

In addition to fullerenes, which have a closed spherical shell composed of sp^2-hybridized carbon atoms, sp^2-hybridized carbon atoms can form one or several coaxial tubes composed of rolled up graphite sheets; they are referred to as carbon nanotubes (CNTs). Such tubes have many valuable properties (electrical conductivity, emission properties) that allow the use of CNTs in biomedical imaging and therapy.[9,10] They can be used as catalyst supports, for creating composite structures, as elements of microelectronics[11] and as carriers of various materials.[12]

At present, a new form of carbon objects — carbon nanoparticles (CNPs) — is of interest. Unlike the above carbon nanomaterials having a highly ordered structure, CNPs are structures containing defects and heterogeneities that largely determine their properties. To date, the scientific community has not yet developed a common opinion on the structure and properties of the CNPs. It is assumed that these nanoobjects do not have a definite shape, but are graphene nanofragments that contain, in addition to hexagonal fragments, defective regions that affect the luminescence properties of CNPs.[13] Because of the lack of a definite shape, the CNPs have a developed defect surface, which also generates interesting luminescent properties.[14]

The unique luminescent properties and simple methods of synthesis of CNPs open up wide prospects for their potential application. There is a growing number of publications on synthetic methods, characteristics and luminescent properties of CNPs, as well as on their biomedical application for cell and tissue imaging, including that *in vivo*.[15–17]

Carbon nanoparticles were accidentally discovered during the purification of carbon nanotubes obtained by the arc discharge method. The interest in CNPs is due to many factors: small particle size, the absence of the need for surface modification, the absence of labourious and costly synthesis steps, the availability of a wide range of starting materials, the absence of toxic components and the simplicity of bioconjugation.[18] Carbon nanoparticles can be synthesized in both polar and nonpolar solvents due to the presence of both hydrophilic and hydrophobic groups on the surface of the particles.[19]

Another important advantage of CNPs is the possibility of their large-scale synthesis from a variety of feedstocks through a wide range of processes (often using a one-step synthesis method and from biological waste), from burning candles and *in situ* dehydration processes to laser ablation techniques.[20–22]

The photoluminescence (PL) of CNPs is characterized by the dependence of the PL spectrum on the excitation wavelength. Carbon nanoparticles are also capable of photoinduced electron transfer, chemiluminescence and electrochemiluminescence.[18] All of these properties make CNPs promising candidates for a new generation of fluorescent biosensors, which can be used in nanobiotechnology and biological science.[23–25] Thus, CNPs are attractive as an alternative to the widely studied 'older generation' carbon materials, such as fullerenes, nanotubes, nanodiamonds and graphene.

Structural analysis demonstrates the similarity of the structures of CNPs obtained by various methods from a variety of materials.[26] Carbon nanoparticles contain a large number of graphene-type carbon–carbon bonds with sp^2 hybrid orbitals of carbon atoms,[14] as well as some number of sp^3-hybridized carbon atoms, which leads to a more disordered structure.[27,28] Nevertheless, the use of different synthesis methods leads to a diverse degree of ordering of graphene fragments in CNPs, as well as to the formation of nanoparticles of different morphologies. For these reasons, the question of the name and classification of CNPs is still open. Cayuela *et al.*[29] proposed the following classification of these structures: carbon nanodots — amorphous quasispherical nanodots that do not show quantum confinement effects; carbon quantum dots (CQDs) — nanoparticles that possess quantum confinement and crystalline structure; graphene quantum dots — π-conjugated graphene nanosheets. Since the quantum-size properties of CNPs have not received sufficient evidence to date, in our opinion, the use of the terms carbon quantum nanodots and carbon nanodots for the entire set of quasispherical carbon nanoparticles is not completely correct. In this review, we mean under CNPs quasispherical nanoparticles obtained from carbon-based compounds, irrespective of the presence of structural and surface defects, or the presence of atoms of other elements. The review does not address ordered carbon nanostructures (graphenes, fullerenes, CNTs) and their luminescent properties.

The following abbreviations are adopted in the review:
TEM — transmission electron microscopy;
AFM — atomic force microscopy;
NMR — nuclear magnetic resonance;
XPS — X-ray photoelectron spectroscopy;
FRET — Förster resonance energy transfer.

II. Methods of synthesis

This section discusses the most common ways of obtaining CNPs and presents the advantages and disadvantages of the proposed methods of synthesis; these data may be of interest to researchers in the field of physical chemistry and carbon materials.

The strategies of synthesis of CNPs can be divided into top-down and bottom-up methods. The top-down strategy makes it possible to produce CNPs from carbon materials, such as graphite, CNTs, carbon black, and carbon oxide.[30] The bottom-up strategy is suitable for synthesizing CNPs from different molecular organic precursors. These methods of synthesis allow one to control the size, shape and properties of the resulting CNPs. However, these approaches frequently have disadvantages associated with complex transformations of a substance during synthesis and a low product yield.[31]

II.1. Top-down methods

II.1.a. Arc discharge

The method is based on the decomposition of large particles of carbon materials into smaller carbon fragments under the action of an electric arc. When purifying single-walled CNTs obtained by arc discharge from soot, Xu *et al.*[32] discovered an unknown luminescent carbon nanomaterial. After boiling in nitric acid and extraction, a black suspension was obtained from which CNPs were isolated. They corresponded to three electrophoretic bands luminescing in

the green-blue, yellow and orange regions of the spectrum. Boiling of CNPs in a solution of oxidant acids is used in most synthesis methods to introduce carboxyl functional groups, increase hydrophilicity and increase the number of defects in the structure of CNPs, which contribute to an increase in PL intensity. The size of CNPs was from 0.5 to 18 nm with predominance of nanoparticles of ~1 nm in diameter.

The disadvantage of this method is the preparation of a mixture of different carbon structures, including the remains of CNTs of various size, which presents a difficulty in purification and separation; therefore, at present this method is practically not used.

II.1.b. Laser ablation

Laser ablation of a carbon substrate is yet another fast way to synthesize CNPs. The advantage of this method is the possibility of obtaining CNPs up to 10 nm in size by evaporation of a carbon material from the target surface as molecules, atoms and ions and their subsequent condensation. Sun's team [28, 33–35] has used laser ablation to produce CNPs. For the ablation of a carbon target (a mixture of graphite powder and cement) in an argon flow, a Nd : YAG laser was used.[28] The particle size was 3 – 10 nm. To increase the PL quantum yield and the stability of CNPs, they were passivated with polymeric agents, such as polyethylene glycol containing terminal amino groups (PEG_{1500N})[28] or poly(propionylethyleneimine-co-ethyleneimine) copolymer.[33] Samples were purified by dialysis; after centrifugation, the CNPs were in the supernatant.[36]

The ultrasonication of a graphite or carbon black dispersion in diethanolamine or PEG_{200N} made it possible to produce CNPs in one stage. The resulting CNPs were ~3.2 nm in size with the interplanar spacing in the crystal lattice within 0.20 – 0.23 nm, analogous to diamond.[34]

Carbon-13-enriched CNPs can be synthesized using a ^{13}C-containing powder as a base; the method afforded CNPs 4 – 5 nm in diameter with a PL quantum yield up to 20%.[37]

A disadvantage of the method is the incomplete use of the target: since evaporation of a carbon material occurs from a narrow erosion zone, the target utilization factor often does not exceed 5%.

II.1.c. Electrochemical methods

Electrochemical methods enable the synthesis of CNPs under mild conditions. Standard electrochemical synthesis is the process of electrochemical etching of various carbon materials, such as graphite, carbon nanotubes and nanofibres, which usually function as electrodes. The key problem of this method is the impossibility of obtaining CNPs with a narrow size distribution due to the difficulty of decomposing the electrode into CNPs of the same size and morphology.[38]

The electrochemical synthesis of CNPs was first carried out by Zhou *et al.*[39] Synthesis was carried out from multilayered carbon nanotubes in the presence of tetra-n-butylammonium ions (TBA^+), which were embedded in the structure of multilayered CNTs, thereby destroying CNTs near these defects to give CNPs. The size of the resulting nanoparticles was from 0.5 to 2.8 nm; they had a maximum emission at ~400 – 500 nm, and a quantum yield of 6.4%.

Another research team[40] synthesized CNPs through oxidation of a graphite electrode at a voltage of 3 V. The resulting solution was purified by centrifugation and then separated into fraction by filtration through membranes with pores of different size. Two fluorescent fractions were separated: with an emission wavelength of 445 nm (pores < 5 kDa) and 510 nm (pores 5 – 10 kDa). It was shown that CNPs had a graphite structure with the interplanar spacing in the crystal lattice of 3.28 Å, which was very close to that for the [002] facet of graphite.

Carbon nanoparticles were synthesized from graphene films used as working electrodes in a phosphate buffer.[41] The resulting CNPs exhibited a green luminescence, were characterized by a narrow size distribution and were stable in an aqueous solution.

The electrochemical production of CNPs cannot always be based on using graphite electrodes as substrates. Deng *et al.*[42] have synthesized CNPs from low-molecular-weight alcohols in an alkaline medium with the use of platinum electrodes. Electrochemical synthesis involves the formation of free radicals, which are cross-linked to give carbon fragments and then dehydration leads to the formation of nanoparticles. The IR spectra of CNPs show bands at 3430, 2930 and 2850 cm^{-1}, which confirm the presence of C – OH and C – H moieties in the structure. The C = O, C = C and C – O – C stretching vibration frequencies are 1700, 1640 and 1250 cm^{-1}, respectively. The PL quantum yield for such CNPs is 15%.

CNPs based on sodium citrate and urea were synthesized by the electrochemical carbonization method.[43] They had high photostability and a high quantum yield of 11.9%. The average size of the resulting nanoparticles was 2.4 nm.

II.2. Bottom-up methods

II.2.a. Hydrothermal synthesis

The hydrothermal method — one of the most popular methods of synthesis of CNPs — is based on heating aqueous (as a rule) solutions of carbon-containing materials in a closed space. This method can lead in one step to surface-modified CNPs with strong luminescence without the need for additional surface passivation and further modification. Among the disadvantages of this method is the possible formation of soot during the synthesis, which can reduce the yield of the product and complicate the purification procedure. Pan *et al.*[44] synthesized CNPs by thermal reduction of single-layer sheets of graphene oxide at 200 – 300 °C for 2 h, followed by oxidation in concentrated acids (H_2SO_4 and HNO_3) under ultrasonication. The average size of the nanoparticles was 10 nm (within 5 – 13 nm). This procedure was improved by Pan *et al.*[23] to obtain CNPs with a narrower size distribution. The hydrothermal synthesis of CNPs from graphene oxide sheets in a strong alkaline medium (pH > 12) afforded CNPs with a smaller average size (3 nm) and a narrower size distribution (1.5 – 5 nm).

Chinese researchers fabricated carbon nanoparticles by the hydrothermal method from solutions of natural carbohydrates (glucose, sucrose, starch) in the presence of hydrochloric acid or sodium hydroxide.[45] Carbohydrate solutions were heated in an autoclave at 160 °C for 4 h. CNPs obtained from different sources had similar morphology and size (70 – 100 nm). The Raman spectra showed two bands: the D peak at ~1340 cm^{-1} and the G peak at

$\sim$1580 cm^{-1}, which are typical of, respectively, sp^2- and sp^3-hybridized carbon atoms.

CNPs have been fabricated by the hydrothermal method from a mixture of citric acid and ethylenediamine followed by dialysis.[46] The resulting particles were 2–6 nm in size and had no pronounced crystal faces. The IR spectra showed C–OH and C–H stretching vibration bands at 3430 and 2923 and 2850 cm^{-1}, respectively; C–NH–C antisymmetric stretching vibration band at 1126 cm^{-1}; N–H bending vibration band at 1570 cm^{-1}; and C=O stretching vibration band at 1635 cm^{-1}.

A mixture of orange juice and ethanol was also used as a carbon source for synthesis of CNPs.[47] The synthesis led to two types of particles: large (30–50 nm) amorphous particles with a relatively weak PL and small (1.5–4.5 nm with an interplanar spacing of 0.18 nm) particles with stronger PL. The PL quantum yields were 20% and 26% for large and small particles, respectively.

CNPs with green, blue and red luminescence were fabricated from *ortho*-, *meta*- and *para*-phenylenediamine, respectively.[48] The synthesis was carried out in an autoclave (180 °C, 12 h) and was followed by purification by column chromatography on silica gel. The particle size was 6.0 (*m*-CNPs), 8.2 (*o*-CNPs) and 10.0 nm (*p*-CNPs).

II.2.b. Microwave synthesis

Microwave synthesis makes it possible to reduce the time of producing CNPs to a few minutes, as well as to vary the size and properties of CNPs by changing the irradiation power and duration. The luminescence quantum yields of CNPs produced by this method are usually lower than those of CNPs synthesized by other methods.[49]

A mixture of citric acid with tetraoctylammonium bromide (TOAB) taken in different concentrations was microwaved for 2–3 min at a power of 500 W.[50,51] The size of CNPs did not exceed 10 nm, and it depended on the TOAB concentration: with increasing concentration, the nanoparticle size decreased. The particles had an amorphous structure (a broad single peak centred at $\sim$20°) with an interplanar spacing of 3.55 Å, which is larger than the distance between the planes in bulk graphite. The IR spectra showed a band at 1750 cm^{-1} corresponding to C=O vibrations, a shoulder at 1650 cm^{-1} corresponding to C=C or $CONH_2$ vibrations and a band at 1200 cm^{-1} caused by –C–O–C– vibrations.

Peng and Travas-Sejdic[52] microwaved carbohydrates in the presence of sulfuric acid; then, the resulting solution was boiled with nitric acid to produce smaller CNPs, neutralized and dialyzed. The CNP surface was treated with 4,7,10-trioxatridecane-1,13-diamine, ethylenediamine, oleylamine or PEG_{1500N}. The size of the resulting CNPs was 5 nm. The IR spectra showed absorption bands at 1572 and 1375 cm^{-1} corresponding to C=C stretching vibrations and C–H bending vibrations, respectively.

Carbon nanoparticles were fabricated using PEG_{200} as the precursor and as the passivating agent.[53] The synthesized CNPs had a relatively high quantum yield ($\sim$16%), which was insensitive to the change in pH.

Zhai *et al.*[54] synthesized CNPs from citric acid in the presence of amines. It has been found that amines can play a dual role — a surface-passivating agent and an agent for introducing nitrogen-containing functional groups. The primary amines showed the greatest efficiency in the synthesis of CNPs, as indicated by the increase in the quantum yield (up to 30% when using ethylenediamine). The IR spectra showed characteristic C=O and C–N stretching vibration bands (1732 and 1580 cm^{-1}, respectively).

II.2.c. Ashing (chemical or thermal oxidation)

This method is an effective approach to the synthesis of CNPs on a large scale. One of the advantages of this method, in addition to the simplicity of obtaining the initial soot for the synthesis of CNPs, is the possibility of its purification from certain metals and their compounds during heating. Particles derived from soot have an average size of <10 nm.[20,27,55] However, this method uses severe conditions for a long time and concentrated acids; as a result, it is possible to prepare CNPs with relatively low quantum yields and poor size distribution.[49]

Mao's research group[20] has prepared CNPs by collecting the combustion soot of candles, which was boiled with nitric acid, analogously to the top-down methods, to increase the number of surface defects and promote surface oxidation. This procedure gave CNPs $\sim$2 nm in diameter. Nanoparticles were purified by dialysis and were fractionated by the gel electrophoresis method. The composition of the purified CNPs (36.8% C, 5.9% H, 9.6% N, 44.7% O) differed significantly from the composition of the initial candle soot (91.7% C, 1.8% H, 1.8% N, 4.4% O); the higher oxygen content can be explained by the presence of surface carbonyl groups.

In further studies, Chen's research team[55] has prepared carbon nanoparticles through natural gas combustion. The resulting soot was boiled with nitric acid, and the CNPs isolated by centrifugation were purified by dialysis. The particle size was 4.8 ± 0.6 nm. ^{13}C NMR and IR spectroscopy pointed to the presence of sp^2-hybridized carbon atoms and carboxyl groups, which led the authors to the conclusion that CNPs consist of a nanocrystalline core based on sp^2-hybridized carbon atoms with a functionalized surface containing carboxyl groups.

The approach to the fabrication of CNPs from human hair has been developed.[56] A mixture of hair and concentrated sulfuric acid was heated at 40, 100 and 140 °C for 24 h. The resulting CNPs had nitrogen- and sulfur-containing functional groups. The quantum yield, elemental composition and optical properties strongly depended on the reaction temperature and the average size of CNPs. Nanoparticles obtained at higher temperatures had a smaller size, contained more sulfur and fluoresced at longer wavelengths.

One of the unique methods is the process of producing CNPs in the absence of heat treatment.[57] The simple mixing of acetic acid, water and phosphorus(V) oxide allowed the preparation of large green fluorescent CNPs stable in aqueous solution. In the course of synthesis, acetic acid serves as a source of carbon, and phosphorus pentoxide acts as a water-removing agent. The average size of CNPs is $\sim$105 nm. It is worth noting that the emission spectrum did not shift with increasing excitation wavelength. In a similar way, glucose-based CNPs were obtained.[58] They also had a large size ($\sim$120 nm), green fluorescence and a low quantum yield ($\sim$8%).

II.2.d. Pyrolysis

The pyrolysis process enables simple and rapid production of CNPs with high PL intensity. Synthesis of CNPs by the pyrolysis of sodium ethylenediaminetetraacetate at 400 °C in a tube furnace under a nitrogen atmosphere has been

described. The resulting black product was sonicated in distilled water to form a brown dispersion, which was further purified.[59] CNPs with a size of ~7.7 nm without visible aggregation were obtained, and the PL quantum yield was 66%.

Low-temperature pyrolysis of citric acid has afforded CNPs with good surface passivation, while the presence of branched polyethyleneimine has made it possible to easily obtain CNPs with a passivated surface and an additional protective layer. The pyrolysis temperature of 200 °C was chosen to prevent the degradation of the protective polymer.[30] In a similar synthesis, *N*-(β-aminoethyl)-γ-aminopropylmethyldimethoxysilane was used for surface passivation.[60] For the synthesis of CNPs, β-cyclodextrin has been calcined in a tube furnace at 300 °C. The resulting black foamed carbon residue was ultrasonicated in nitric acid, treated in a microwave oven and then purified. Calcination of sodium glutamate in an oven at 400 °C, followed by grinding of the prepared material and purification by dispersing two times gave CNPs with PL in various spectral regions.[61]

II.2.e. Matrix synthesis

The above methods of synthesis of CNPs do not allow one to control the size of the nanoparticles obtained. The use of special matrices that serve as a template for CNPs makes it possible to adjust the size more accurately. Initially, organic reactants are located on the surface or in the cavity (pores) of nanoreactors; then, they are subjected to high-temperature treatment. The disadvantage of the method is the need to separate the resulting CNPs from matrices.[49]

Liu *et al.*[62] used, as matrices, silicon microspheres with a surface modified with surfactants. As a result, the polymerization occurred on the surface of silicon matrices rather than in solution. Heating at 900 °C produced CNPs/SiO_2 particles, the silicon matrix was removed, and the resulting CNPs had an amorphous structure and a size of 1.5 – 2.5 nm. The particles were oxidized with nitric acid and passivated by treatment with PEG_{1500N}.

Silicon matrices as nanoreactors have also been used for synthesizing CNPs from glycerol and PEG_{NH_2}.[63] Silicon matrices were mixed with the reactants and heated at 230 °C for 30 min, and the final product was isolated by centrifugation. The resulting CNPs had a narrow size distribution in the range 3.0 ± 0.3 nm.

In another approach used by Giannelis and coworkers,[64] zeolites served as matrices. First, zeolites were subjected to ion exchange with 2,4-diaminophenol hydrochloride with subsequent thermal oxidation. Then, the matrix material was etched out with hydrofluoric acid to give CNPs 4 – 6 nm in size.

Many of the above methods have a number of drawbacks, such as low yield of the target product, soot formation, and production of CNPs that are heterogeneous in composition and morphology. Therefore, the search for high-performance methods for synthesis and fractionation of CNPs is of great importance. As shown in Table 1, pyrolysis makes it possible to obtain CNPs with sufficiently high quantum yield. In many cases, the quantum yield can be increased by the addition of passivating agents, such as PEG, ethylenediamine and oleylamine. The size of the particles as a whole does not depend on the synthesis method (top-down and bottom-up), but in the top-down methods it is especially difficult to control the size of the resulting CNPs, because the degradation of the starting material occurs nonuniformly. Therefore, the bottom-up methods are believed to be more convenient for the synthesis of particles of similar morphology.

III. Study of properties

Due to the relative novelty and complexity of carbon nanoparticles, the study of their chemical nature and properties requires the use of various physical and chemical methods of investigation. Since CNPs exhibit interesting optical properties, numerous studies are aimed at trying to explain the mechanisms of photophysical phenomena arising in these carbon nanoparticles.

III.1. Absorption in the UV/Vis range

Absorption of light in the ultraviolet and visible range of the optical spectrum (UV/Vis absorption) is caused by electronic transitions. CNPs obtained by different methods absorb UV light, with the position of the absorption peak depending on the conditions of particle synthesis.

The absorption spectra of CNPs obtained by laser ablation from a carbon target[28] have no pronounced peak (Fig. 1). In the case of CNPs prepared by electrochemical synthesis from multilayered CNTs,[39] the spectra showed an intense and narrow absorption peak at a wavelength of 270 nm (4.59 eV). The authors attributed this fact to the narrow size distribution of the resulting particles (2.8 ± 0.5 nm). The absorption spectra of CNPs synthesized electrochemically from graphite showed a small peak at a wavelength of 300 nm.[40, 65] The absorption spectra of CNPs obtained from graphene sheets through a hydrothermal route showed, in addition to the peak at 230 nm ($\pi \rightarrow \pi^*$ transition of aromatic sp^2 domains) present in the spectra of initial graphene fragments, a new peak at 320 nm associated with the formation of CNPs.[44]

Li *et al.*[59] have studied the effect of temperature of the hydrothermal synthesis of CNPs from a mixture of citric acid and ethylenediamine on the photophysical properties of the resulting CNPs. The synthesis was carried out in the temperature range from 150 to 300 °C in 50 °C increment. The absorption spectrum of the four types of CNPs showed two peaks: at 240 nm (assigned to the emission of the carbon core), whose intensity increased for the samples synthesized at a higher temperature, and at 344 nm (assigned to the emission of molecular fragments and surface structures), whose intensity, on the contrary, decreased for the samples synthesized at a higher temperature. The authors attributed this to an increase in the degree of carbonization of CNPs with increasing the synthesis temperature. Consequently, the structures obtained at low temperatures are predominantly converted to carbon ones formed at high temperatures.

The absorption spectra of CNPs synthesized by a hydrothermal method from orange juice showed a broad band at 288 nm, which was attributed to energy transitions of aromatic π-orbitals in the sample.[47] In the spectra of three types of CNPs produced from phenylenediamine isomers, a red shift of absorption bands with respect to their positions for the starting compounds was observed.[48] According to the authors, the displacement of electronic transitions is evidence that the synthesized CNPs have a smaller band gap width than the starting phenylenediamine isomers.

Table 1. Methods of synthesis and properties of the synthesized carbon nanoparticles.

Synthesis method	Starting material/ passivating agent (if any)	Nanoparticle size /nm	Quantum yield (%)	Composition (%)	PL colour or emission wavelength /nm	Ref.
			Top-down methods			
Arc discharge	CNTs	0.5 – 18	1.6 [a]	53.9 C, 2.6 H, 1.2 N, 40.3 O	Green-blue, yellow, orange	32
Laser ablation	Graphite powder/PEG_{1500N}	5	4 – 10	–	480 – 650	28
	Graphite powder/PEG_{200N}	3.2	3 – 8	–	500	34
	Carbon powder ^{13}C / PEG_{1500N}	4 – 5	$\leqslant$20	–	Green	37
Electro-	Graphite electrode	2.8 ± 0.5	6.4	–	450	39
chemical		1.9 ± 0.3	–	–	445	40
synthesis		3.2 ± 0.5	–	–	510	40
	Graphene film	3 – 5	–	–	Green/470	41
	Low-molecular-weight alcohols	2.1 – 4.3	15.9	80.5 C, 1.7 H, 0.8 N	400 – 570	42
	Sodium citrate, urea	1.0 – 3.5	11.9	–	420 – 550	43
			Bottom-up methods			
Hydrothermal synthesis	Graphene oxide	5 – 13	–	–	43	44
	Glucose, sucrose, starch	70 – 100	–	59.2 C, 4.2 H, 36.6 O	450 – 460	45
	Citric acid	2 – 6	60	–	443	46
	Orange juice	30 – 50	20	–	474	47
		1.5 – 4.5	26	–	455	47
	m-Phenylenediamine	6.0	10.4	–	435	48
	o-Phenylenediamine	8.2	17.6	–	535	48
	p-Phenylenediamine	10.0	26.1	–	604	48
Microwave synthesis	Citric acid	5 – 10	–	–	350 – 600	50
	Carbohydrate material/ 4,7,10-trioxatridecane-1,13-diamine, ethylenediamine, oleylamine, PEG_{1500N}	5	–	57.0 C, 7.5 H, 80.5 N, 27.0 O	420 – 520	52
	Citric acid/amines	2.2 – 3.2 [b]	30.2 [b]	53.4 C, 6.0 H, 20.2 N [b]	420 – 550 [b]	54
	PEG_{200}	4.5 ± 0.9	16		450 – 600	53
Ashing	Candle soot	2	0.8	36.8 C, 5.9 H,	415	20
			1.9	9.6 N, 44.7	495	20
			0.8		577	20
	Soot after natural gas combustion	4.8 ± 0.6	–	–	420 – 470	55
	Human hair	4 – 10	9	61.2 C, 5.4 N, 2.1 S	383	56
		2 – 7	16	59.7 C, 5.4 N, 4.0 S	450	56
		2 – 5	29	60.6 C, 5.6 N, 5.1 S	470	56
	Acetic acid	105			Green	57
	Glucose	120	8	48.9 C, 4.8 H, 46.3 O	450	58

Table 1 (continued).

Synthesis method	Starting material/ passivating agent (if any)	Nanoparticle size /nm	Quantum yield (%)	Composition (%)	PL colour or emission wavelength /nm	Ref.
		Bottom-up methods				
Pyrolysis	Sodium ethylenediamine-tetraacetate	7.7	66	–	400 – 480	59
	Citric acid/polyethyleneimine	15 – 18	–	–	550 – 650	30
Matrix synthesis	Surfactant F127/PEG_{1500N}	1.5 – 2.5	–	–	420 – 600	62
	Glycerol/ PEG_{NH_2}	3.0 ± 0.3	32	–	450 – 480	63
	Citric acid	5 – 10	–	–	350 – 600	50

[a] For yellow CNPs; [b] when ethylenediamine is used.

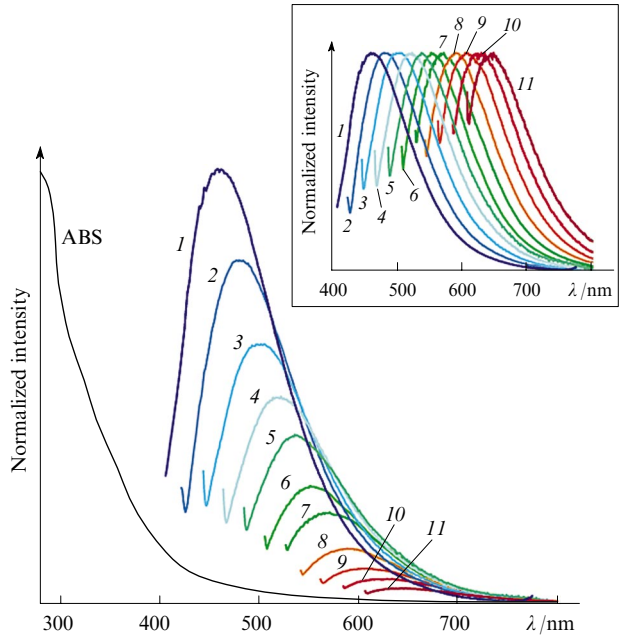


Figure 1. Absorption spectrum (ABS) and excitation-dependent photoluminescence spectra CNPs.[28]
The excitation wavelength was changed from 400 (curve *1*) to 600 nm (curve *11*) in 20 nm increment.

III.2. Photoluminescence

Excitation-dependent photoluminescence, a wide spectral range and relatively strong emission bands can be considered the most interesting properties of CNPs. Whereas the PL colour of semiconductor quantum dots is related to quantum-size effects and, thus, correlates with the nanoparticle diameter, the PL peak position can be explained by other properties. Available synthetic procedures afford CNPs of different sizes; however, the excitation-dependent emission (see Fig. 1) is probably associated with the appearance of new energy states of nanoparticles arising from the presence of surface defects of CNPs. With a decrease in the number of defects, especially on the CNP surface, it is presumably possible to reduce the dependence of the PL spectrum on the excitation wavelength.[66] The CNPs obtained by different methods basically exhibit excitation-dependent PL, with the emission band lying in the blue-green region of the spectrum. Some of researchers have managed to obtain CNPs with longer-wavelength emission [28] and/or with emission at the same wavelength.[48]

In addition, an important characteristic of CNPs is the quantum yield. In particular, CNPs obtained by laser ablation showed wavelength-dependent PL in the excitation wavelength range from 400 to 600 nm, with a quantum yield of these particles ranging from 4% to 10%.[28] The excitation-dependent PL was also observed for CNPs synthesized by Zhou *et al.*[39] The excitation range for these particles was from 360 to 500 nm. The quantum yield was calculated with respect to quinine sulfate (quantum yield of 54%) and anthracene (quantum yield of 27%). The quantum yield of CNPs was 6.3 ± 1.0%. The photoluminescence of CNPs obtained electrochemically from graphene sheets depended on the wavelength and was observed at excitation wavelengths in the range from 320 to 420 nm.[44] The quantum yield, calculated with respect to quinine sulfate, was 6.9%. The CNPs obtained by the hydrothermal method from citric acid were characterized by a excitation-dependent PL in the excitation wavelength range from 300 to 460 nm.[46] The PL quantum yield of CNPs increased from 17% to 75% with an increase in the synthesis temperature from 150 to 300 °C. Carbon nanoparticles obtained by the hydrothermal method from orange juice [47] exhibited excitation-dependent PL in the excitation wavelength range 320 – 450 nm, the quantum yield was 25.6%. MW-assisted synthesis has led to CNPs with excitation-dependent PL in the excitation range 340 – 460 nm and a quantum yield of 6.3%.[50]

Jiang *et al.*[48] have described the production of three types of CNPs from phenylenediamine isomers with constant positions of the blue, green and red PL peaks. Excitation of CNPs at a wavelength of 365 nm led to emission at λ = 4435 (*m*-CNPs), 535 (*o*-CNPs) and 604 nm (*p*-CNPs). In order to increase the PL intensity of CNPs in the green and red regions, the optimal excitation wavelengths are λ = 420 and 510 nm, respectively. The quantum yield for *m*-CNPs was calculated with respect to quinine sulfate for a wavelength of 365 nm and was 4.8%. The quantum yield for *o*-CNPs was calculated with respect to Rhodamine 6G for a wavelength of 365 nm (10.4%) and for a more suitable wavelength of 420 nm (17.6%). The quantum yield for *p*-CNPs was calculated with respect to Rhod-

amine B and amounted to 20.6% for a wavelength of 365 nm and 26.1%for a more suitable wavelength of 510 nm.

III.3. Other methods of investigation

From the point of view of luminescent and physicochemical properties, the size distribution of CNPs, the internal structure of CNPs (their crystallinity), the presence of defects and impurities as well as surface properties, such as the charge and presence of defects and functional groups are of interest.

The presence of luminescent properties of CNPs over a wide wavelength range prevents the use of the dynamic light scattering method, which is commonly used for studying the dimensions and surface charge of nanoparticles, and forces researchers to resort to various variants of electron and probe microscopy.

Transmission electron microscopy (TEM), high resolution TEM (HRTEM) and atomic force microscopy (AFM) are the most widely used techniques in the study of CNPs. The TEM method makes it possible to see a solid core and obtain a size distribution of a sufficiently large ensemble of particles. HRTEM makes it possible to characterize the internal structure of CNPs (layers of carbon atoms). The AFM method visualizes not only the inner solid core, but also the outer soft shells of polymer-passivated CNPs, and can also estimate the three-dimensional particle shape. The widespread use of atomic force microscopes with fully digital controllers, where the analogue-to-digital conversion of signals occurs with high resolution and speed as near as possible to the probe position recording system, has made it possible to significantly improve the signal-to-noise ratio and, as a result, to obtain a high-quality image of individual nanoparticles with resolution comparable to that in the TEM method. The small size of CNPs requires the use of supersharp probes based on whiskers and diamond-like structures. In Russia, most widely used are the so-called Klinov cantilevers [67] with a tip formed by a set of individual diamond-like whiskers. The typical radius of such a tip can reach 1 nm (for comparison, the tip radius of standard silicon probes is $\sim$3 nm). Since the shape of the particles in the measurement will be distorted by convolution with the shape of the probe, a deconvolution operation in determining the true size of the CNPs is necessary during post-processing, for example, using Villarrubia's blind evaluation algorithm.[68] If CNPs lie on the surface of a solid substrate with distances greater than the probe size, this method gives good results.

To study the internal structure and assess the crystallinity, X-ray diffraction analysis, NMR and Raman spectroscopy are used in addition to HRTEM.

The X-ray diffraction analysis provides information on the unit cell parameters in crystalline carbon cores and sheds light on the presence of a certain type of crystal lattice in the structure of the particles. The diffraction peak at 20° frequently observed in the diffraction patterns of CNPs indicates the presence of the graphite crystal structure.[66]

The NMR method makes it possible to obtain information on the type of hybridization of carbon atoms in crystal lattices and the order of the bonds between them and, hence, more fully characterizes the structure of synthesized CNPs.

For a typical Raman spectrum of carbon nanoparticles, the presence of D and G modes is characteristic, and the presence of 2D modes is also possible. The D peak at $\sim$1350 cm^{-1}, corresponding to the vibrations of disordered sp^2-hybridized carbon atoms, appears in the spectra of samples with a large number of structural defects. The G peak at $\sim$1580 cm^{-1} refers to the tangential stretching vibrations of the C–C bond and is associated with the doubly degenerate phonon mode of symmetry E_{2g} at the centre of the Brillouin zone.[66] The 2D peak at $\sim$2710 cm^{-1} appears in graphite structures under resonance light scattering involving two phonons with the same energy, but with the opposite direction of the momentum, and gives information on the ordering of the graphite layers. The intensity ratio of characteristic Raman peaks (I_D/I_G) can be used to study the structural properties of CNPs, in particular, the degree of crystallinity and the relative ratio of carbon atoms within particles and at the surface. The disadvantages of the Raman spectroscopy include the strong influence of PL on the recorded spectra, which can be avoided by using a metal substrate to quench the luminescence of relatively small nanometre-sized particles or a laser with a longer wavelength whose quantum energy is smaller than the longest wavelength electron transition for CNPs. In particular, a laser with a wavelength of 633 nm was used to record the Raman spectrum for CNPs, but the PL of the sample had a significant effect on the result so that the expected peaks were not observed (Fig. 2 *a*) [46]; the D and G peaks of the CNPs have been detected [47] (see Fig. 2 *b*).

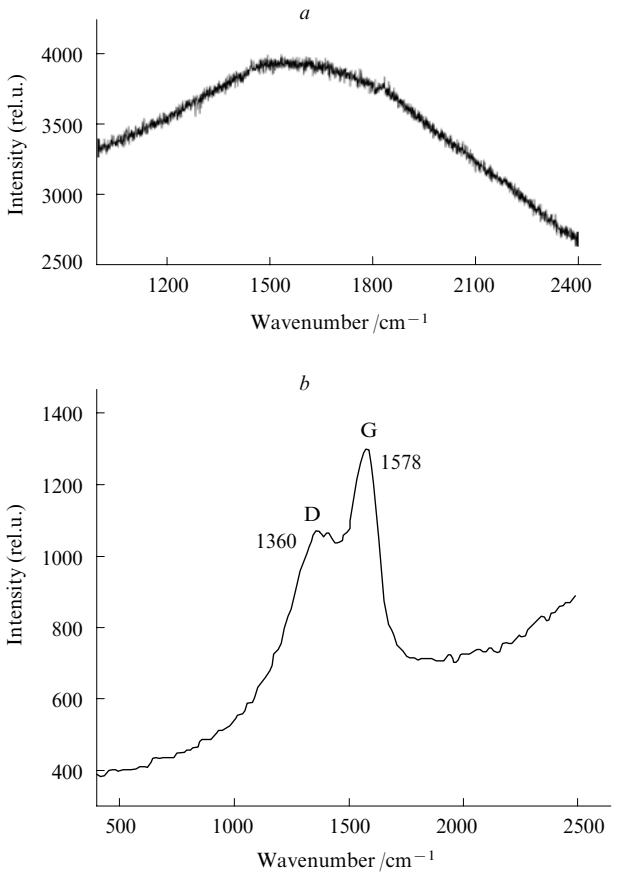


Figure 2. Raman spectra for CNPs distorted by the superimposed strong PL (*a*) [46] and Raman spectrum of the CNP fraction distorted by the superimposed weaker PL (*b*).[47]

To study the surface of the CNPs and determine the functional groups that affect the appearance of new energy states and, consequently, the nature of PL, the Fourier transform IR (FTIR) spectroscopy and X-ray photoelectron spectroscopy (XPS) methods are used.

FTIR spectroscopy is complementary to the Raman spectroscopy method, but, unlike the latter one, IR-active are asymmetric vibrations with a change in dipole moment. The method makes it possible to study the samples in the gaseous, liquid and solid state, but the use of water as a solvent is impossible because of the broad peaks of water absorption in the IR range. There are oxygen-containing carboxylic, hydroxyl, epoxy and ester functional groups on the CNP surface, which are observed in the FTIR spectra of CNPs.[66]

The XPS method makes it possible to obtain information on the chemical and electronic state of the atoms present on the CNP surface. Spectrum analysis makes it possible to calculate the quantitative ratio of atoms in matter, and when a high-resolution method (for example, based on the N1s, O1s and C1s spectra) is used, it reveals the presence of different types of atomic environment. FTIR spectroscopy and XPS often complement each other, which provides a more complete characterization of functional groups on the surface of samples and, thus, a better understanding of the causes of PL in a certain wavelength range.

In particular, Jiang *et al.*[48] failed to detect significant differences in the IR spectra of CNPs with blue, green and red PL obtained from the phenylenediamine isomers (Fig. 3). These spectra showed new lines in the ranges 2848 – 2920, 1336 – 1384 and 1225 – 1234 cm^{-1} for all three types of CNPs compared to the starting compounds. The authors explained this by the appearance of C – H, C – N=

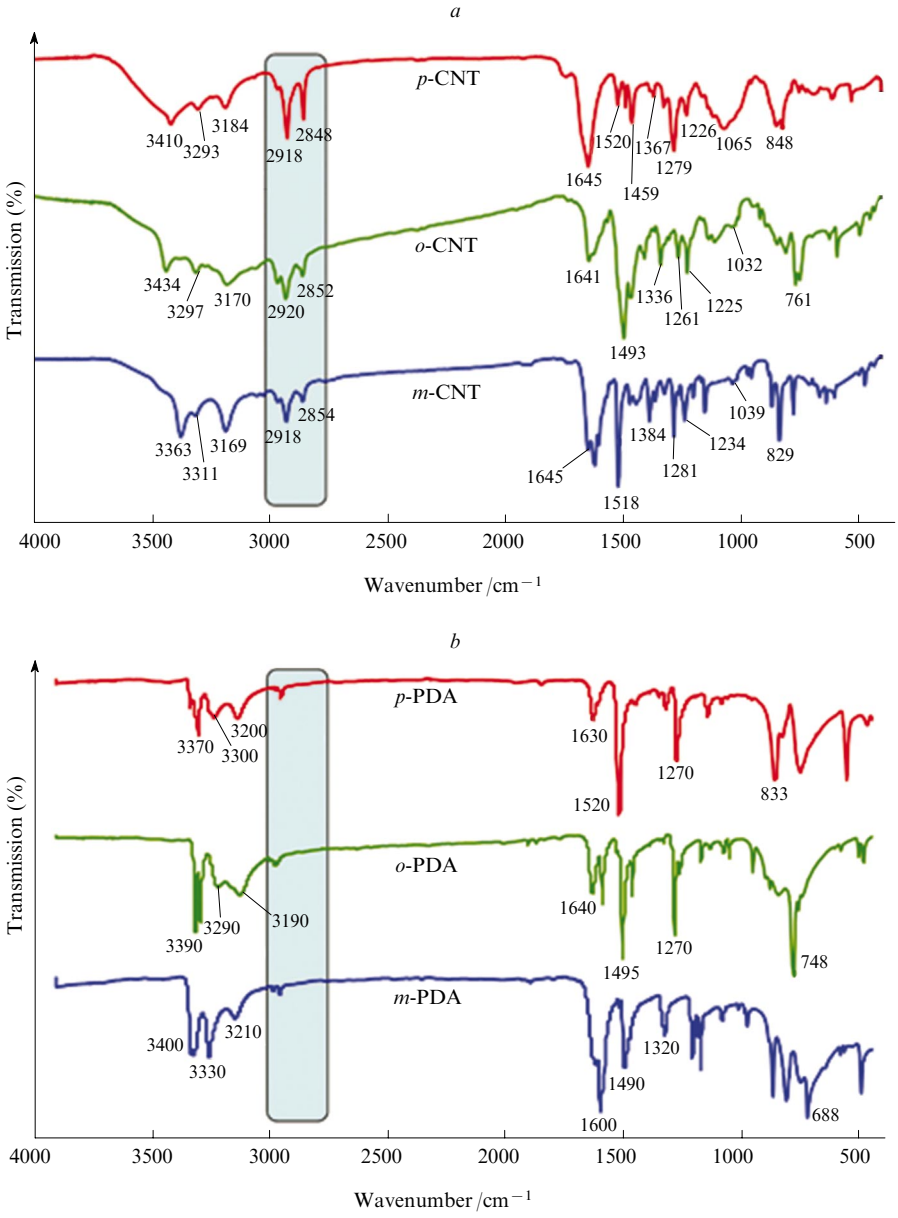


Figure 3. FTIR spectra of CNPs (*a*) and starting phenylenediamine (PDA) isomers (*b*).[48]

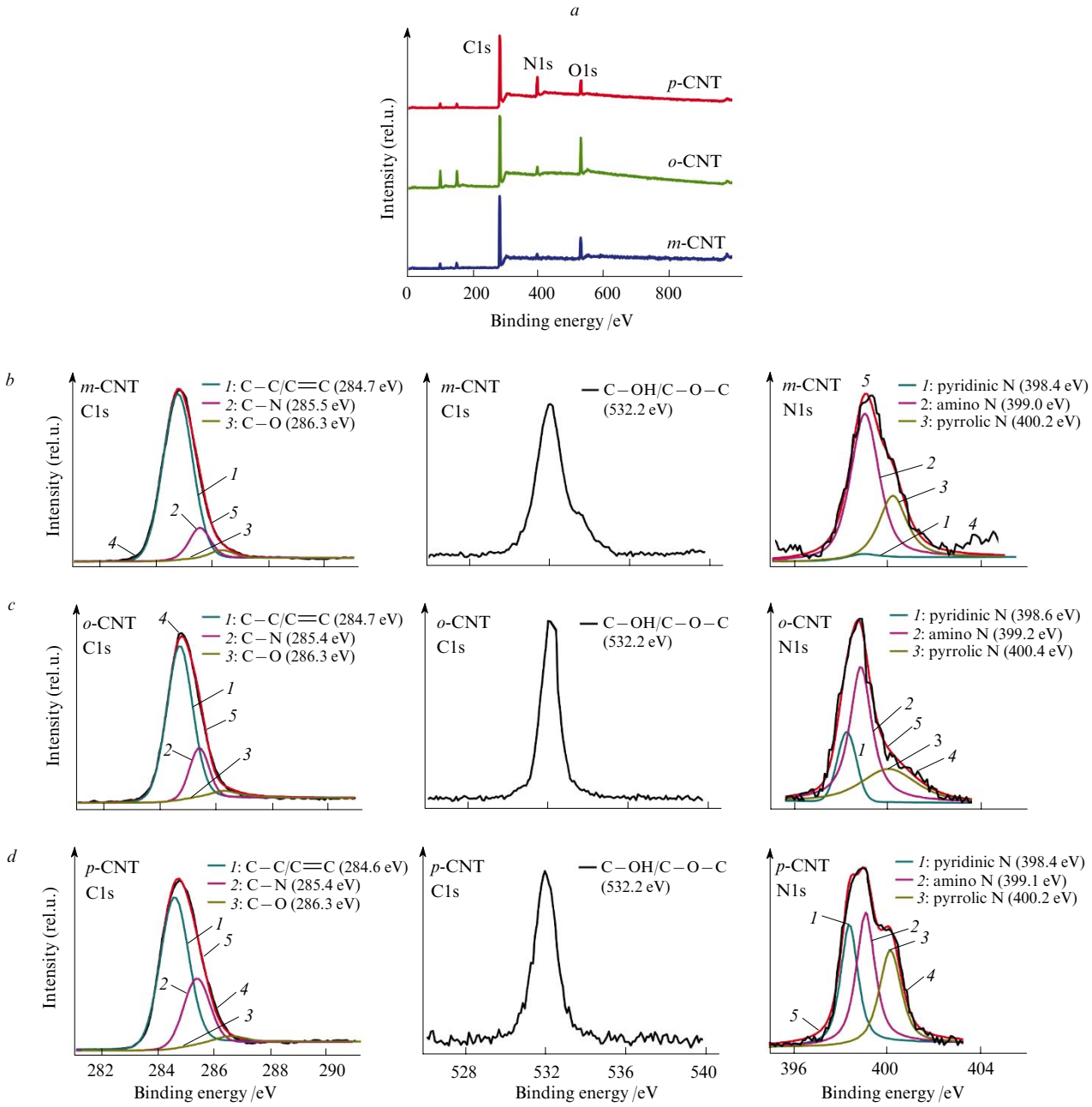


Figure 4. XPS spectra of *m*-, *o*- and *p*-CNPs (*a*). The C1s spectra (left and central panels) and the N1s spectra (right panel) of *m*-CNPs (*b*), *o*-CNPs (*c*) and *p*-CNPs (*d*).[48]
Lines *4* (——) and *5* (——) in the C1s and N1s spectra are, respectively, raw data and fitted line.

and C–O stretching vibrations, respectively, and assumed that the formation of CNPs was accompanied by decomposition, intermolecular cyclization and condensation. The XPS analysis made it possible to identify the differences between the samples (Fig. 4). According to the results of this analysis, all samples contained the same chemical bonds [from the C1s spectra, C–C and C=C (284.7 eV), C–N (285.5 eV), C–O (286.3 eV), C–OH and C–O–C (532.2 eV) bonds were found; the N1s spectra revealed the presence of a nitrogen atom in the pyridine group (398.6 eV) and in the amino group (399.0 eV) as well as in the pyrrole moiety (400.2 eV). (400.2 eV)].The differences are in the content of nitrogen atoms (3.69%, 7.32% and 15.57% for *m*-CNPs, *o*-CNPs and *p*-CNPs, respectively) and in the ratio of various N-containing moieties in the samples. The authors believe that such a difference partly determines the different character of PL of these samples.

IV. Application in biology and medicine

This section considers the use of CNPs for biomedical purposes, since the toxicity and size of the agents used are particularly important in this area. Since carbon is the main element of living organisms, carbon nanomaterials are

characterized by low toxicity compared to other nanomaterials. Carbon nanoparticles do not contain heavy metals in their structure, as do widely known semiconductor quantum dots; therefore, they are not able to provoke health and environmental problems.[69] They have a size on the nanometre scale and, therefore, are convenient for the introduction into a cell *in vivo*. In addition, the surface of CNPs contains a variety of functional groups and can be modified by organic, inorganic, polymeric and other substances exhibiting different properties.[70]

IV.1. Application in chemical analysis

Carbon nanoparticles are widely used due to their solubility in water and high photochemical and chemical stability. Interaction of CNPs with metal ions often leads to luminescence quenching. This effect is due to coordination interactions between metal ions and functional groups on the surface of CNPs. Nanoparticles with different surface groups can respond to different metal ions.[71]

It has been shown [72, 73] that the PL properties of CNP solution are sensitive to the presence of Hg^{2+} ions. As PL probes, surface-passivated CNPs obtained by laser ablation have been used. The photoluminescence of these particles is efficiently quenched in the presence of micromolar amounts of Hg^{2+} (the Stern – Volmer quenching rate constant is 1.3×10^5 litre mol^{-1}). A significant improvement in sensitivity has been achieved with the use of CNPs containing nitrogen atoms (the Stern – Volmer quenching constant increased by two orders of magnitude and amounted to 1.4×10^7 litre mol^{-1}), presumably due to the presence of CN groups on the CNP surface.

In addition, the use of CNPs allows one to selectively detect the presence of Hg^{2+} ions in living cells. CNPs with a quantum yield of 65.5% and 55.4%, respectively, were obtained on the basis of citric acid and ethylene-1,2-diamine or *N*-(β-aminoethyl)-γ-aminopropylmethyldimethoxysilane.[74] Adding 20 μmol of Hg^{2+} decreases the PL intensity of CNPs by 80% and 50% respectively; both systems are stable after 1 h of observation. The PL quenching is reversible: the emission intensity is restored by the addition of a strong chelating agent, such as EDTA, so that the CNPs can serve as probes with reversible PL quenching.[74] Carbon nanoparticles have been used to detect metal ions, such as Cu^{2+} (Ref. 75), Fe^{3+} (Ref. 76), Pb^{2+} (Ref. 77), Cr^{VI} (Ref. 78) and Ag^{+} (Ref. 79).

Selective determination of 2,4,6-trinitrotoluene (TNT) ions in aqueous solution by means of Förster resonance energy transfer (FRET) due to the π – π-stacking interaction between CNPs and aromatic rings in the structure of TNT has been described.[80] Using 1 ml of a solution of CNPs without additional modification enables the detection of TNT in concentrations down to 2.2 mol $litre^{-1}$.

In addition to the use of traditional PL of CNPs as an analytical signal, recent studies have shown the applicability of chemiluminescence,[81] in particular, for the detection of NO_2,[82] and electrochemiluminescence [83] for the determination of traces of pentachlorophenol [84] and Cu^{2+} (Ref. 85), Fe^{3+} (Ref. 86) and Pb^{2+} (Ref. 87).

Carbon nanoparticles conjugated with antibodies can be used as biolabels. Based on the principles of FRET and homogeneous immunoassay,[88] a biosensor has been proposed for the rapid and specific determination of 4,4′-dibromobiphenyl — a persistent organic contaminant that disrupts the endocrine system.[89] The immunosensor consists of gold nanoparticles functionalized with antibodies specific to 4,4′-dibromobiphenyl and CNPs labelled with 4,4′-dibromobiphenyl antigen, which function as acceptors and donors, respectively. As a result of energy transfer, the PL of CNPs is efficiently quenched with gold nanoparticles. In the presence of 4,4′-dibromobiphenyl, CNPs labelled with antigen are released from the surface of gold nanoparticles due to competing immunoreaction with PL recovery.

It has been shown that CNPs bound to dye molecules are efficient indicators for H_2S. The presence of H_2S traces initiates energy transfer, leading to a change in the PL colour of CNPs from blue to green.[90] Carbon nanoparticles synthesized using *N*-(β-aminoethyl)-γ-aminopropylmethyldimethoxysilane as the carbon source selectively bind to Cu^{2+} ions due to the presence of ethylenediamine groups on their surface. Dual-emission structures have been obtained by fixing such CNPs on the surface of Rhodamine B-doped silica nanoparticles. Cu^{2+} ions efficiently quenched the PL of CNPs, while their effect on the luminescence of Rhodamine B was insignificant. These systems were successfully applied for the *in vivo* imaging of Cu^{2+} in living cells.[91]

When using CNPs produced from glutamic acid by pyrolysis for detection of amoxicillin, Niu and Gao [92] have demonstrated that amoxicillin molecules efficiently separate CNPs from each other and thus decrease the nonradiative transitions, which ultimately enhances the PL intensity.[92] The use of CNPs for detection of other low-molecular-weight bioanalytes, such as dopamine,[93] ascorbic acid [78] and glucose [94] has been reported.

IV.2. Visualization

Carbon nanoparticles are promising as an alternative to semiconductor quantum dots for *in vitro* and *in vivo* imaging of biological systems.[95, 96] It has been shown that surface-passivated low-toxicity CNPs can safely be used in high concentrations for *in vivo* imaging. PEG-coated CNPs had no toxic effects *in vivo* for 28 days upon intravenous administration to mice at a dose of 8 – 40 mg kg^{-1}. Physiological indices were the same in all mice receiving various doses of CNPs, indicating the expected nontoxicity of CNPs at the given and lower dosages commonly used for *in vivo* imaging. No abnormalities were found in the organs examined for the study, despite the fact that the concentration of CNPs in the liver and spleen was higher than in the other organs.[37] In addition, the cell viability after treatment with CNPs at various concentrations has been studied. It has been found that the average cell viability is >95% at a concentration of CNPs not exceeding 1.8 mg ml^{-1}. These results clearly show that CNPs are much more biocompatible than semiconductor quantum dots.[18, 64]

The localization of CNPs in cells is largely determined by the properties of their surface. Particles passivated with the poly(propionylethylenimine-co-ethylenimine) copolymer and synthesized from activated carbon can serve as labels for the cell membrane and cytoplasm of MCF-7 and COS-7 cells.[33, 97, 98] At the same time, cells incubated with silica-coated CNPs demonstrated a bright PL only in the cytoplasmic region.[99] CNPs coated with an amphiphilic biocompatible polymer have been synthesized and proved to be capable of penetrating the membrane and accumulating in the cytosol.[100]

Before imaging, cells are usually incubated with CNPs to ensure cell uptake of the latter. It was suggested that CNPs move into the cell through endocytosis. In addition,

the uptake of CNPs, presumably, can be improved by their binding to membrane-permeating proteins.[101, 102]

As mentioned above, CNPs are capable of luminescing in different wavelength ranges, which allows researchers to monitor and select emission and excitation wavelengths.[60] If the excitation wavelength is sufficiently shifted into the red region of the spectrum, CNPs are able to emit in the near-IR range. Despite the fact that the emission in the near-IR spectral region is relatively weak, CNPs have a great potential for working in the field of biotissue transparency.[103] The possibility of using CNPs as contrast agents in living mice has been demonstrated.[104] In experiments, PEG_{1500N}-passivated CNPs were administered to mice subcutaneously, which resulted in a bright PL, decaying only after 24 h. In the case of intravenous administration of CNPs, PL was observed only in the bladder region, confirming that urination is the main way of excretion of intravenously administered CNPs.

Carbon nanoparticles coated with ZnS were used for *in vivo* imaging in mice,[105] demonstrating the PL brightness comparable to that of the CdSe/ZnS quantum dots. However, after subcutaneous administration of CNPs and CdSe/ZnS quantum dots to mice, it was found that, although both types of nanoparticles moved to axillary lymph nodes, the former moved much more slowly than the latter.[106] The reason for this was the presence of PEG molecules on the surface of CNPs, which weakened the interaction between CNPs and lymphatic cells. Of particular interest was the observed competitive performance of the CNPs *in vivo* to that of the CdSe/ZnS quantum dots. The results suggest that CNPs may be further developed into a new class of high-performance and nontoxic contrast agents for optical bioimaging.[106]

Despite the fact that CNPs are currently used for imaging objects not only *in vitro*, but also *in vivo*, the photoluminescence of most CNPs is in the UV or short-wavelength visible region, which significantly limits the use of CNPs for deep tissue monitoring. In addition, almost all organisms have autoluminescence in the same spectral ranges, which can seriously affect the results of the study. Therefore, it is necessary to create CNPs that have near-IR luminescence.[70]

IV.3. Nanomedicine

Carbon nanoparticles can be used in photodynamic therapy for the treatment of superficial tumours.[104] First, CNPs are localized in tumour tissue and, then, they are exposed to light at a specific wavelength that causes the formation of singlet oxygen acting on cancer cells. It was found that CNPs have an inhibitory effect on MCF-7 and MDA-MB-231 cells.

Juzenas *et al.*[107] used polymer-functionalized CNPs. When irradiated with UV light, the CNPs showed a significant photodynamic effect towards the Du145 and PC3 cell lines. One of the most popular semiconductor photocatalysts is TiO_2, but this photocatalyst can be excited only in the UV range.[108] The UV radiation has a low penetrating power and is not able to penetrate deep into the skin.[109] As compared to TiO_2, CNPs have the advantage of having the tunable band gap: the band gap width can be reduced in order to excite CNPs with radiation at wavelengths capable of penetrating deeper into the tissue.

The platform for photodynamic therapy was developed by adding a photosensitizer (chlorin e6) to CNPs.[110] It has been demonstrated that CNPs can excite a photosensitizer by the FRET mechanism. It has been shown that the PL

Table 2. Examples of analytical, biological and medicinal applications of carbon nanoparticles.

Synthesis method	Starting substance	Emission wavelength /nm	Application	Ref.
Laser ablation	Carbon target	450	Detection of Hg^{2+}	74
Microwaving	Glucose	452	Detection of Cu^{2+}	75
Electrochemical	Graphite rod	445	Detection of Fe^{3+}	76
Ashing	Starch	400	Detection of Pb^{2+}	77
Ashing	Graphite sheets	450 – 600	Quantification of 2,4,6-trinitrotoluene	80
Hydrothermal	*N*-(β-amnioethyl)-γ-amino-propylmethyldimethoxysilane	467, 585	Quantification of Cu^{2+}	94
Pyrolysis	Glutamic acid	470	Quantification of amoxicillin	92
Hydrothermal	Citric acid	480	Quantification of dopamine	93
Microwaving	Organic amines: dimethylamine, ethylamine, tripropylamine	480	Quantification of glucose	94
Laser ablation	Carbon target	480 – 800	Labelling of breast cancer MCF-7 cells	33
Pyrolysis	Green tea	360 – 530	Labelling of MCF-7, MCF-10 A and MDA-MB-231 cancer cells	97
Ashing	Activated carbon	430 – 550	Labelling of COS-7 cells	98
Arc discharge	Graphite rod	450	Photodynamic effect for Du145 and PC3 cells	107
Laser ablation	Carbon target	470, 525	Photodynamic therapy	110
		430	The same	111

resulting from two-photon absorption is potentially useful for the treatment of deep tumours.[111] Excitation of CNPs at a wavelength of 800 nm became possible due to binding the photosensitizer (protoporphyrin IX) to CNPs and excitation of the latter through energy transfer. This allowed excitation to be carried out in the transparency window when the exciting light can penetrate into human tissue four times deeper than light with $\lambda = 630$ nm used in photodynamic therapy.

Zheng *et al.*[112] conjugated CNPs with an anticancer platinum(VI)-based prodrug — oxidized oxaliplatin. The resulting conjugate was taken up by cancer cells through endocytosis; then, the drug was released after reduction under the action of a strongly basic medium in cancer cells. It was also shown that the distribution of the drug bound to CNPs could be monitored by photoluminescence of CNPs, thereby controlling the time of drug administration and dosage.

Table 2 summarizes data on the application of CNPs in various fields. It can be noted that the synthesis methods and starting materials do not affect the area of application of CNPs. Carbon nanoparticles are synthesized by various methods, many of which include post-treatment with modifying agents to achieve the necessary surface functionalization. For biomedical purposes, CNPs with an emission wavelength of ~ 500 nm are most commonly used, but the emission wavelength can be shifted in the production of an analytical signal, for example, by the FRET mechanism.

V. Conclusion

Since the discovery of luminescent CNPs in 2004, more than ten years have passed, during which they have been studied in various ways. Numerous approaches to the synthesis of CNPs and modification of their structure have been proposed, purification and fractionation techniques have been developed, and the field of application of CNPs has been extended. Carbon nanoparticles are characterized by photo- and chemical stability and low toxicity for cells and living organisms; therefore, biology and medicine have become the main fields of their application. In biomedical applications, CNPs have significant potential as a nontoxic substitute for traditional quantum dots.

However, an understanding of the structure and properties of CNPs, especially their relationship, is still far from being complete. The variety of methods for producing CNPs and the large number of starting materials that are used for their synthesis cause a wide variety of properties and characteristics of CNPs. Small deviations from the synthesis procedure or the presence of impurities in the starting materials lead to a significant variation in structure and properties. Such variations have serious consequences, since the luminescence characteristics strongly depend on the composition of CNPs and on the amount and nature of the functional groups on their surface. To obtain luminescent CNPs with reproducible properties, it is necessary to elucidate the factors determining the composition and structure of the particles formed, as well as the mechanisms of the effect of composition and structure on luminescent properties.

In this context, the main attention should be given, in our opinion, to the following issues: the fabrication of CNPs with reproducible parameters, small size and high quantum yield as a result of improving the methods of synthesis and passivation of the CNP surface or separation and purification, as well as the understanding of the photoluminescence process, since this will facilitate the use of CNPs in the field of biology and medicine, especially *in vivo*.

This review was written with the financial support of the Russian Science Foundation (Project No. 16-13-10195).

Figure 1 is reproduced with permission of the © 2006 American Chemical Society. Figure 2 *a* is reproduced with permission of the © 2015 Wiley-VCH Verlag. Figure 2 *b* is reproduced with permission of © 2012 The Royal Society of Chemistry. Figure 3 is reproduced with permission of the © 2015 Wiley-VCH Verlag. Figure 4 is reproduced with permission of the © 2015 Wiley-VCH Verlag.

References

1. G Jia, H Wang, L Yan, X Wang, R Pei, T Yan, Y Zhao, X Guo *Environ. Sci. Technol.* **39** 1378 (2005)
2. V Georgakilas, J A Perman, J Tucek, R Zboril *Chem. Rev.* **115** 4744 (2015)
3. K B Ghiassi, M M Olmstead, A L Balch *Dalton Trans.* **43** 7346 (2014)
4. T Y Zakharian, A Seryshev, B Sitharaman, B E Gilbert, V Knight, L J Wilson *J. Am. Chem. Soc.* **127** 12508 (2005)
5. K Iakoubovskii, M V Baidakova, B H Wouters, A Stesmans, G J Adriaenssens, A Y Vul', P J Grobet *Diamond Relat. Mater.* **9** 861 (2000)
6. S-J Yu, M-W Kang, H-C Chang, K-M Chen, Y-C Yu *J. Am. Chem. Soc.* **127** 17604 (2005)
7. X Kong, L C L Huang, S-C V Liau, C-C Han, H-C Chang *Anal. Chem.* **77** 4273 (2005)
8. J-I Chao, E Perevedentseva, P-H Chung, K-K Liu, C-Y Cheng, C-C Chang, C-L Cheng *Biophys. J.* **93** 2199 (2007)
9. T Murakami, H Nakatsuji, M Inada, Y Matoba, T Umeyama, M Tsujimoto, S Isoda, M Hashida, H Imahori *J. Am. Chem. Soc.* **134** 17862 (2012)
10. J T Robinson, K Welsher, S M Tabakman, S P Sherlock, H Wang, R Luong, H Dai *Nano Res.* **3** 779 (2010)
11. M F L De Volder, S H Tawfick, R H Baughman, A J Hart *Science* **339** 535 (2013)
12. E Katz, I Willner *ChemPhysChem* **5** 1084 (2004)
13. M O Dekaliuk, O Viagin, Y V Malyukin, A P Demchenko *Phys. Chem. Chem. Phys.* **16** 16075 (2014)
14. G Hong, S Diao, A L Antaris, H Dai *Chem. Rev.* **115** 10816 (2015)
15. T Feng, X Ai, G An, P Yang, Y Zhao *ACS Nano* **10** 4410 (2016)
16. M Zheng, S Ruan, S Liu, T Sun, D Qu, H Zhao, Z Xie, H Gao, X Jing, Z Sun *ACS Nano* **9** 11455 (2015)
17. J Wen, Y Xu, H Li, A Lu, S Sun *Chem. Commun.* **51** 11346 (2015)
18. S N Baker, G A Baker *Angew. Chem., Int. Ed.* **49** 6726 (2010)
19. O Kozák, K K R Datta, M Greplová, V Ranc, J Kašlík, R Zbořil *J. Phys. Chem. C* **117** 24991 (2013)
20. H Liu, T Ye, C Mao *Angew. Chem., Int. Ed.* **46** 6473 (2007)
21. L Tang, R Ji, X Cao, J Lin, H Jiang, X Li, K S Teng, C M Luk, S Zeng, J Hao, S P Lau *ACS Nano* **6** 5102 (2012)
22. H M R Gonçalves, A J Duarte, F Davis, S P J Higson, J C G Esteves da Silva *Anal. Chim. Acta* **735** 90 (2012)
23. D Pan, L Guo, J Zhang, C Xi, Q Xue, H Huang, J Li, Z Zhang, W Yu, Z Chen, Z Li, M Wu *J. Mater. Chem.* **22** 3314 (2012)
24. H Tao, K Yang, Z Ma, J Wan, Y Zhang, Z Kang, Z Liu *Small* **8** 281 (2012)
25. J Tang, B Kong, H Wu, M Xu, Yo Wang, Ya Wang, D Zhao, G Zheng *Adv. Mater.* **25** 6569 (2013)

26. A P Demchenko, M O Dekaliuk *Methods Appl. Fluoresc.* **1** 042001 (2013)
27. S C Ray, A Saha, N R Jana, R Sarkar *J. Phys. Chem. C* **113** 18546 (2009)
28. Y-P Sun, B Zhou, Y Lin, W Wang, K A S Fernando, P Pathak, M J Meziani, B A Harruff, X Wang, H Wang, P G Luo, H Yang, M E Kose, B Chen, L M Veca, S-Y Xie *J. Am. Chem. Soc.* **128** 7756 (2006)
29. A Cayuela, M L Soriano, C Carrillo-Carrión, M Valcárcel *Chem. Commun.* **52** 1311 (2016)
30. Y Dong, R Wang, H Li, J Shao, Y Chi, X Lin, G Chen *Carbon* **50** 2810 (2012)
31. A Ananthanarayanan, X Wang, P Routh, B Sana, S Lim, D-H Kim, K-H Lim, J Li, P Chen *Adv. Funct. Mater.* **24** 3021 (2014)
32. X Xu, R Ray, Y Gu, H J Ploehn, L Gearheart, K Raker, W A Scrivens *J. Am. Chem. Soc.* **126** 12736 (2004)
33. L Cao, X Wang, M J Meziani, F Lu, H Wang, P G Luo, Y Lin, B A Harruff, L M Veca, D Murray, S-Y Xie, Y-P Sun *J. Am. Chem. Soc.* **129** 11318 (2007)
34. S-L Hu, K-Y Niu, J Sun, J Yang, N-Q Zhao, X-W Du *J. Mater. Chem.* **19** 484 (2009)
35. X Wang, L Cao, F Lu, M J Meziani, H Li, G Qi, B Zhou, B A Harruff, F Kermarrec, Y-P Sun *Chem. Commun.* 3774 (2009)
36. Y-P Sun, X Wang, F Lu, L Cao, M J Meziani, P G Luo, L Gu, L M Veca *J. Phys. Chem. C* **112** 18295 (2008)
37. S-T Yang, X Wang, H Wang, F Lu, P G Luo, L Cao, M J Meziani, J-H Liu, Y Liu, M Chen, Y Huang, Y-P Sun *J. Phys. Chem. C* **113** 18110 (2009)
38. B-P Qi, L Bao, Z-L Zhang, D-W Pang *ACS Appl. Mater. Interfaces* **8** 28372 (2016)
39. J Zhou, C Booker, R Li, X Zhou, T-K Sham, X Sun, Z Ding *J. Am. Chem. Soc.* **129** 744 (2007)
40. Q-L Zhao, Z-L Zhang, B-H Huang, J Peng, M Zhang, D-W Pang *Chem. Commun.* 5116 (2008)
41. Y Li, Y Hu, Y Zhao, G Shi, L Deng, Y Hou, L Qu *Adv. Mater.* **23** 776 (2011)
42. J Deng, Q Lu, N Mi, H Li, M Liu, M Xu, L Tan, Q Xie, Y Zhang, S Yao *Chem. – Eur. J.* **20** 4993 (2014)
43. Y Hou, Q Lu, J Deng, H Li, Y Zhang *Anal. Chim. Acta* **866** 69 (2015)
44. D Pan, J Zhang, Z Li, M Wu *Adv. Mater.* **22** 734 (2010)
45. X He, H Li, Y Liu, H Huang, Z Kang, S-T Lee *Colloids Surf., B* **87** 326 (2011)
46. S Zhu, Q Meng, L Wang, J Zhang, Y Song, H Jin, K Zhang, H Sun, H Wang, B Yang *Angew. Chem., Int. Ed.* **52** 3953 (2013)
47. S Sahu, B Behera, T K Maiti, S Mohapatra *Chem. Commun.* **48** 8835 (2012)
48. K Jiang, S Sun, L Zhang, Y Lu, A Wu, C Cai, H Lin *Angew. Chem., Int. Ed.* **54** 5360 (2015)
49. A Das, P T Snee *ChemPhysChem* **17** 598 (2016)
50. H Zhu, X Wang, Y Li, Z Wang, F Yang, X Yang *Chem. Commun.* 5118 (2009)
51. M L Bhaisare, A Talib, M S Khan, S Pandey, H-F Wu *Microchim. Acta* **182** 2173 (2015)
52. H Peng, J Travas-Sejdic *Chem. Mater.* **21** 5563 (2009)
53. A Jaiswal, S S Ghosh, A Chattopadhyay *Chem. Commun.* **48** 407 (2012)
54. X Zhai, P Zhang, C Liu, T Bai, W Li, L Dai, W Liu *Chem. Commun.* **48** 7955 (2012)
55. L Tian, D Ghosh, W Chen, S Pradhan, X Chang, S Chen *Chem. Mater.* **21** 2803 (2009)
56. D Sun, R Ban, P-H Zhang, G-H Wu, J-R Zhang, J-J Zhu *Carbon* **64** 424 (2013)
57. Y Fang, S Guo, D Li, C Zhu, W Ren, S Dong, E Wang *ACS Nano* **6** 400 (2012)
58. P Zuo, D Xiao, M Gao, J Peng, R Pan, Y Xia, H He *Microchim. Acta* **181** 1309 (2014)
59. X Li, J Chang, F Xu, X Wang, Y Lang, Z Gao, D Wu, K Jiang *Res. Chem. Intermed.* **41** 813 (2015)
60. C Liu, P Zhang, X Zhai, F Tian, W Li, J Yang, Y Liu, H Wang, W Wang, W Liu *Biomaterials* **33** 3604 (2012)
61. N Zheng, S Ding, X Zhou *Colloids Surf., B* **142** 123 (2016)
62. R Liu, D Wu, S Liu, K Koynov, W Knoll, Q Li *Angew. Chem., Int. Ed.* **48** 4598 (2009)
63. C-W Lai, Y-H Hsiao, Y-K Peng, P-T Chou *J. Mater. Chem.* **22** 14403 (2012)
64. A B Bourlinos, A Stassinopoulos, D Anglos, R Zboril, V Georgakilas, E P Giannelis *Chem. Mater.* **20** 4539 (2008)
65. L Zheng, Y Chi, Y Dong, J Lin, B Wang *J. Am. Chem. Soc.* **131** 4564 (2009)
66. R Jelinek *Carbon Quantum Dots*. Springer Cham 2017
67. D V Klinov, T V Neretina, V V Prokhorov, T V Dobrynina, K G Aldarov, V V Demin *Biochemistry* **74** 1150 (2009)
68. J S Villarrubia *J. Res. Natl. Inst. Stand. Technol.* **102** 425 (1997)
69. W Wang, L Cheng, W Liu *Sci. China Chem.* **57** 522 (2014)
70. J Zuo, T Jiang, X Zhao, X Xiong, S Xiao, Z Zhu *J. Nanomater.* **2015** 1 (2015)
71. Y Dong, J Cai, X You, Y Chi *Analyst* **140** 7468 (2015)
72. H M R GonUalves, A J Duarte, J C G Esteves da Silva *Biosens. Bioelectron.* **26** 1302 (2010)
73. S Y Lim, W Shen, Z Gao *Chem. Soc. Rev.* **44** 362 (2015)
74. F Yan, Y Zou, M Wang, X Mu, N Yang, L Chen *Sens. Actuators, B: Chem.* **192** 488 (2014)
75. J-M Liu, L Lin, X-X Wang, S-Q Lin, W-L Cai, L-H Zhang, Z-Y Zheng *Analyst* **137** 2637 (2012)
76. Y-L Zhang, L Wang, H-C Zhang, Y Liu, H-Y Wang, Z-H Kang, S-T Lee *RSC Adv.* **3** 3733 (2013)
77. S S Wee, Y H Ng, S M Ng *Talanta* **116** 71 (2013)
78. M Zheng, Z Xie, D Qu, D Li, P Du, X Jing, Z Sun *ACS Appl. Mater. Interfaces* **5** 13242 (2013)
79. Z Qian, J Ma, X Shan, H Feng, L Shao, J Chen *Chem. – Eur. J.* **20** 2254 (2014)
80. L Fan, Y Hu, X Wang, L Zhang, F Li, D Han, Z Li, Q Zhang, Z Wang, L Niu *Talanta* **101** 192 (2012)
81. Z Lin, W Xue, H Chen, J-M Lin *Chem. Commun.* **48** 1051 (2012)
82. Z Lin, X Dou, H Li, Y Ma, J-M Lin *Talanta* **132** 457 (2015)
83. Y Xu, J Liu, C Gao, E Wang *Electrochem. Commun.* **48** 151 (2014)
84. J Li, N Wang, T Tran, T C Huang, L Chen, L Yuan, L Zhou, R Shen, Q Cai *Analyst* **138** 2038 (2013)
85. Y Xu, M Wu, X-Z Feng, X-B Yin, X-W He, Y-K Zhang *Chem. – Eur. J.* **19** 6282 (2013)
86. P Zhang, Z Xue, D Luo, W Yu, Z Guo, T Wang *Anal. Chem.* **86** 5620 (2014)
87. Y Dong, W Tian, S Ren, R Dai, Y Chi, G Chen *ACS Appl. Mater. Interfaces* **6** 1646 (2014)
88. D Bu, H Zhuang, G Yang, X Ping *Sens. Actuators, B: Chem.* **195** 540 (2014)
89. T Hyötyläinen, K Hartonen *TrAC, Trends Anal. Chem.* **21** 13 (2002)
90. C Yu, X Li, F Zeng, F Zheng, S Wu *Chem. Commun.* **49** 403 (2013)
91. X Liu, N Zhang, T Bing, D Shangguan *Anal. Chem.* **86** 2289 (2014)
92. J Niu, H Gao *J. Lumin.* **149** 159 (2014)
93. Y Mao, Y Bao, D Han, F Li, L Niu *Biosens. Bioelectron.* **38** 55 (2012)
94. S Liu, J Tian, L Wang, Y Luo, X Sun *RSC Adv.* **2** 411 (2012)
95. V N Mehta, S Jha, R K Singhal, S K Kailasa *New J. Chem.* **38** 6152 (2014)
96. J Wang, J Qiu *J. Mater. Sci.* **51** 4728 (2016)

97. P-C Hsu, P-C Chen, C-M Ou, H-Y Chang, H-T Chang *J. Mater. Chem. B* **1** 1774 (2013)
98. Z-A Qiao, Y Wang, Y Gao, H Li, T Dai, Y Liu, Q Huo *Chem. Commun.* **46** 8812 (2010)
99. F Wang, Z Xie, H Zhang, C Liu, Y Zhang *Adv. Funct. Mater.* **21** 1027 (2011)
100. C Fowley, B McCaughan, A Devlin, I Yildiz, F M Raymo, J F Callan *Chem. Commun.* 9361 (2012)
101. S Santra, H Yang, J T Stanley, P H Holloway, B M Moudgil, G Walter, R A Mericle *Chem. Commun.* **25** 3144 (2005)
102. M Stroh, J P Zimmer, D G Duda, T S Levchenko, K S Cohen, E B Brown, D T Scadden, V P Torchilin, M G Bawendi, D Fukumura, R K Jain *Nat. Med.* **11** 678 (2005)
103. H Ding, L-W Cheng, Y-Y Ma, J-L Kong, H-M Xiong *New J. Chem.* **37** 2515 (2013)
104. D Bechet, P Couleaud, C Frochot, M-L Viriot, F Guillemin, M Barberi-Heyob *Trends Biotechnol.* **26** 612 (2008)
105. L Cao, S-T Yang, X Wang, P G Luo, J-H Liu, S Sahu, Y Liu, Y-P Sun *Theranostics* **2** 295 (2012)
106. H Li, X He, Z Kang, H Huang, Y Liu, J Liu, S Lian, C H A Tsang, X Yang, S-T Lee *Angew. Chem., Int. Ed.* **49** 4430 (2010)
107. P Juzenas, A Kleinauskas, P G Luo, Y-P Sun *Appl. Phys. Lett.* **103** 063701 (2013)
108. S N Frank, A J Bard *J. Phys. Chem.* **81** 1484 (1977)
109. K P Nielsen, A Juzeniene, P Juzenas, K Stamnes, J J Stamnes, J Moan *Photochem. Photobiol.* **81** 1190 (2005)
110. P Huang, J Lin, X Wang, Z Wang, C Zhang, M He, K Wang, F Chen, Z Li, G Shen, D Cui, X Chen *Adv. Mater.* **24** 5104 (2012)
111. C Fowley, N Nomikou, A P McHale, B McCaughan, J F Callan *Chem. Commun.* **49** 8934 (2013)
112. M Zheng, S Liu, J Li, D Qu, H Zhao, X Guan, X Hu, Z Xie, X Jing, Z Sun *Adv. Mater.* **26** 3554 (2014)